

In-situ identification of copper-based green pigments on paintings and manuscripts by reflection FTIR

D. Buti · F. Rosi · B. G. Brunetti · C. Miliani

Received: 23 October 2012 / Revised: 24 December 2012 / Accepted: 4 January 2013 / Published online: 23 January 2013
© Springer-Verlag Berlin Heidelberg 2013

Abstract In this work non-invasive reflection infrared spectroscopy was used to discriminate between different Cu-based green pigments (namely, malachite, verdigris, chrysocolla, emerald green and phthalo green). The pigments, chosen because of their historical widespread use in artworks, were investigated as pure powders and in situ on painted models by reflection FTIR spectroscopy. The distortion arising as a result of the specular and diffuse component of reflected radiation was evaluated as function of the optical and surface properties of the investigated mock-ups. Use of the Kramers–Kronig (KK) algorithm to correct for the distortion arising from the surface reflection gave k index maxima shifted by more than 20 cm^{-1} relative to those obtained in conventional transmission mode. These findings stress the need to carefully manage use of the KK algorithm on reflection spectra to avoid erroneous assignment. On the other hand, combination and overtone bands (which are enhanced by the diffuse reflection) were proved to enable reliable and sensitive identification of most of the pigments studied. Knowledge acquired by study of pure compounds

and painted models was subsequently applied to interpret the spectra acquired from paintings and manuscripts.

Keywords Cu-based green pigments · Mid and near IR reflection · Kramers–Kronig conversion · Combination and overtone bands · Non-invasive analysis

Introduction

In recent years there has been an exponential increase of interest in the use of non-invasive analytical techniques able to yield information by non-contact examination of entire artwork surfaces [1]. A multi-technique approach based on the use of complementary spectroscopies (i.e. X-ray fluorescence, Raman, FTIR, UV–visible absorption and emission) proved very effective for identification of artists' palettes for different types of artworks, from mural paintings [2] to easel paintings [3], and from illuminated manuscripts [4] to ceramics and glasses [5]. Despite the good results obtained for blue [3, 6], white [7, 8], yellow [3, 9], and red [10, 11] pigments, very often the non-invasive approach has proved to be quite unspecific for green compounds [3, 12–15], mainly copper-based. Copper-based green pigments are a large class of pigments characterized by the presence of copper (II) in octahedral coordination which is responsible for the coloration via d–d electronic transition. All copper-based green pigments give similar results when analysed by elemental analysis and electronic spectroscopy, because the key element, copper, is non-fluorescent and always furnishes a similar absorption band centred at approximately 600 nm; use of molecular structural spectroscopy (for example FTIR, Raman, or X-ray diffraction) is, therefore, advisable for effective discrimination among these compounds. For the sake of completeness it must be mentioned that other types of green pigments are available

D. Buti · F. Rosi · B. G. Brunetti · C. Miliani (✉)
Centro di Eccellenza SMAArt (Scientific Methodologies applied to Archaeology and Art), c/o Dipartimento di Chimica, Università degli Studi di Perugia, Via Elce di Sotto 8, 06123 Perugia, Italy
e-mail: miliani@thch.unipg.it

D. Buti
Dipartimento di Chimica, Università di Firenze, Polo Scientifico, Via della Lastruccia 3, 50019 Sesto Fiorentino, Firenze, Italy

F. Rosi · B. G. Brunetti · C. Miliani
Istituto CNR-ISTM (Istituto di Scienze e Tecnologie Molecolari), c/o Dipartimento di Chimica, Università degli Studi di Perugia, Via Elce di Sotto 8, 06123 Perugia, Italy

to artists, for example green earth (clays containing Fe^{2+}), viridian (chromium oxide), and vergaut (a mixture of indigo and orpiment).

In the work discussed in this paper reflection FTIR spectroscopy was used for non-invasive identification of green Cu-based pigments in different types of artwork. Five copper-based green pigments were selected on the basis of their occurrence in artwork (as summarized in Table 1) and also on the basis of their molecular structure, to enable study of different types of copper ligands. These compounds were studied by focusing the attention on their spectral response in reflection infrared spectroscopy, alone as a pressed powder and when mixed with organic binders as model paintings.

Reflection infrared spectroscopy generally implies a normal optical layout ($0^\circ/0^\circ$ geometry) thus theoretically favouring the collection of the specular reflected light. In practice, both the surface roughness of the object and the infrared optical properties of the investigated materials may generate light containing both diffuse-like volume and specular-like surface reflections. As a consequence, the two competing components of reflection (i.e. specular and diffuse) lead to different spectral distortions, and thus to challenges in spectral interpretation [20]. Surface reflection obeys Fresnel's law [21] which correlates the reflected light with both the refraction and absorption indexes. According to this law, for low absorption index bands the reflection profile follows mainly the derivative-like behaviour of the refraction index, resulting in inflection points in the corresponding infrared reflectance spectrum. Conversely, high absorption index bands are totally reflected and appear as inverted or so-called *reststrahlen* bands [21].

Band shift and broadening, and an increase in the combination and overtone bands, are generated by the volume reflection [20]. The forbidden combination and overtone bands, which have a lower absorption index, are, in fact, largely crossed by the light resulting in higher

effective sample thickness. For this reason they are not usually distorted but instead enhanced in reflection mode compared with the stronger bands. The diagnostic usefulness of the undistorted combination and overtone bands has already been demonstrated for a variety of pigments [20, 22]. Interpretation of the distorted features generated by the infrared total reflection is challenging and, quite often, the Kramers–Kronig (KK) algorithm is used to obtain more conventional spectral profiles [23, 24]; this is, however, not correct when both contributions (specular and diffuse) are present [21].

The effects of diffuse and specular reflection on the spectral features of each pigment have been considered; this has enabled determination of diagnostic peaks which can be used for identification of copper-based pigments on paintings and manuscripts by non-invasive FTIR spectroscopy.

Experimental

Materials

Laboratory samples were prepared with commercial artists' pigments (malachite, verdigris, and chrysocolla from Zecchi, Florence, Italy; phthalo green from Maimeri, Milan, Italy; emerald green from Kremer Pigmente, Aichstetten, Germany) and binding media (cold pressed linseed oil, casein, and animal glue from Zecchi).

Painting mock-ups were prepared for each green pigment. The lipid binder used was linseed oil (oil models) whereas for the proteinaceous binder (tempera models) all pigments were mixed with casein, with the exception of verdigris which, having low affinity for casein, was applied with animal glue. Linseed oil was mixed directly with pigment whereas casein and animal glue were diluted with alkaline water. For each pigment, a 2:1 pigment-to-binder weight ratio was used, with the exception of the phthalocyanine green oil mock-up, for

Table 1 Name, chemical formula, and historical context of use of the copper-based green pigments analysed in this work

Pigment	Formula	Historical use
Malachite	$\text{CuCO}_3 \cdot \text{Cu(OH)}_2$ basic copper carbonate [16]	Used in Egypt for eye-paint since predynastic times (before 3200 BC). Then used in paintings during the Greek and Roman period; finally in European easel painting in the XVth and XVIth centuries. Malachite has also been found in Western Chinese paintings of the IXth to Xth centuries [16]
Verdigris ^a	$\text{Cu(CH}_3\text{COO)}_2 \cdot \text{H}_2\text{O}/\text{Cu(CH}_3\text{COO)}_2 \cdot 3\text{Cu(OH)}_2 \cdot 2\text{H}_2\text{O}$ neutral and/or basic copper acetate [17]	Used since the Roman Age (mentioned by Pliny in his <i>Naturalis Historia</i>). Widely used in the Middle Ages, the Renaissance, and the baroque period [17]
Chrysocolla	$(\text{Cu, Al})_2\text{H}_2\text{Si}_2\text{O}_5(\text{OH})_4 \cdot n\text{H}_2\text{O}$ copper silicate [18]	Used in Ancient Egypt (since the Predynastic period), India, and China [18]
Emerald green	$3\text{Cu(AsO}_2)_2 \cdot \text{Cu(CH}_3\text{COO)}_2$ copper acetoarsenite [19]	Discovered between 1800 and 1814. Used until the end of the XIXth century. Popular among the French impressionist and post-impressionist artists [19]
Phthalo green	$\text{C}_{32}\text{H}_2\text{N}_8\text{Cl}_{14}\text{Cu}$ chlorate phthalocyanine [18]	Discovered in the 1907 and used from the 1930s as both painting and restoration material [18]

^a In this work a neutral copper acetate was used

which a 1:1 pigment-to-binder ratio was used. These ratios resulted in the best fluid yet thick consistency suitable for painting. Only for malachite were prepared further models with different pigment-to-binder weight ratios (1:2, 1:1, 2:1, and 3:1), to estimate spectral interference from the binders and the detection limit of the pigment for diagnostic purposes. The paint model samples were kept in the dark and at ambient temperature for approximately six months before being measured.

The results obtained from the study of the laboratory samples were finally used for interpretation of the spectra collected in situ on real artworks through the MOLAB transnational access [1] founded by the Eu-ARTECH (FP6) and CHARISMA (FP7) European projects.

Spectra acquired in total reflection mode from the following artworks (painted with malachite, emerald green, and verdigris) were selected as examples for discussion:

- two illuminated Gospels conserved in the Putna Monastery (Romania);
- a manuscript of the XV century belonging to the library of Palazzo Corsini (Accademia dei Lincei in Rome, Italy);
- *Adorazione dei Pastori* (1522), a mural painting by Perugino (Madonna delle Lagrime Church, Trevi, Italy);
- *Polittico di Sant'Angelo* (1499), an altarpiece by Niccolò di Liberatore (Sant'Angelo Church, Bastia Umbra, Italy);
- *The Crucifixion of Christ* (1855–1893), Ethiopian painting on canvas (British Museum, London);
- *Chemistry* (1909–11), painting on canvas by Edvard Munch (Aula of Oslo University, Oslo, Norway); and
- *Dinamismo di un corpo umano* (1913), a painting on canvas by Umberto Boccioni (Museo del Novecento, Milan, Italy).

Infrared transmission spectroscopy

Transmission mid-FTIR spectra were recorded by use of a Jasco FT/IR-470 plus spectrophotometer, comprising a Global IR radiation source, a Michelson interferometer, and a pyroelectric deuterated triglycine sulfate (DTGS) detector. Spectra were collected in KBr (Sigma–Aldrich, Steinheim, Germany) pellets in the range 400–4000 cm^{-1} , with a spectral resolution of 2 cm^{-1} .

Infrared reflection spectroscopy

Reflection mid-FTIR spectra were recorded by use of a portable Jasco VIR 9500 spectrophotometer equipped with a Remspec mid-infrared fibre optic sampling probe. The instrumentation is made up of a Midac Illuminator IR radiation source, a Michelson interferometer, and a liquid nitrogen-cooled MCT detector. Measurements were

collected with a bifurcated cable probe containing 19 chalcogenide glass fibres that enabled collection of spectra in the range 6000–900 cm^{-1} . The probe diameter was approximately 4 mm. Total reflectivity, R , i.e. the combined diffuse and specular components, was collected over 800 scans, at a resolution of 4 cm^{-1} , using the spectrum from an aluminium mirror plate for background correction. Spectra were expressed as function of pseudo-absorbance A' where $A' = \log(1/R)$. Kramers–Kronig transformation was applied in the 7000–900 cm^{-1} spectral range, by using the routine available in Jasco software version 1.53.04.

Reflection spectra of pure copper-compounds were collected from pellets prepared with 1 g pigment without dilution. Pigments, because of their different grain size, were ground before compression.

Results and discussion

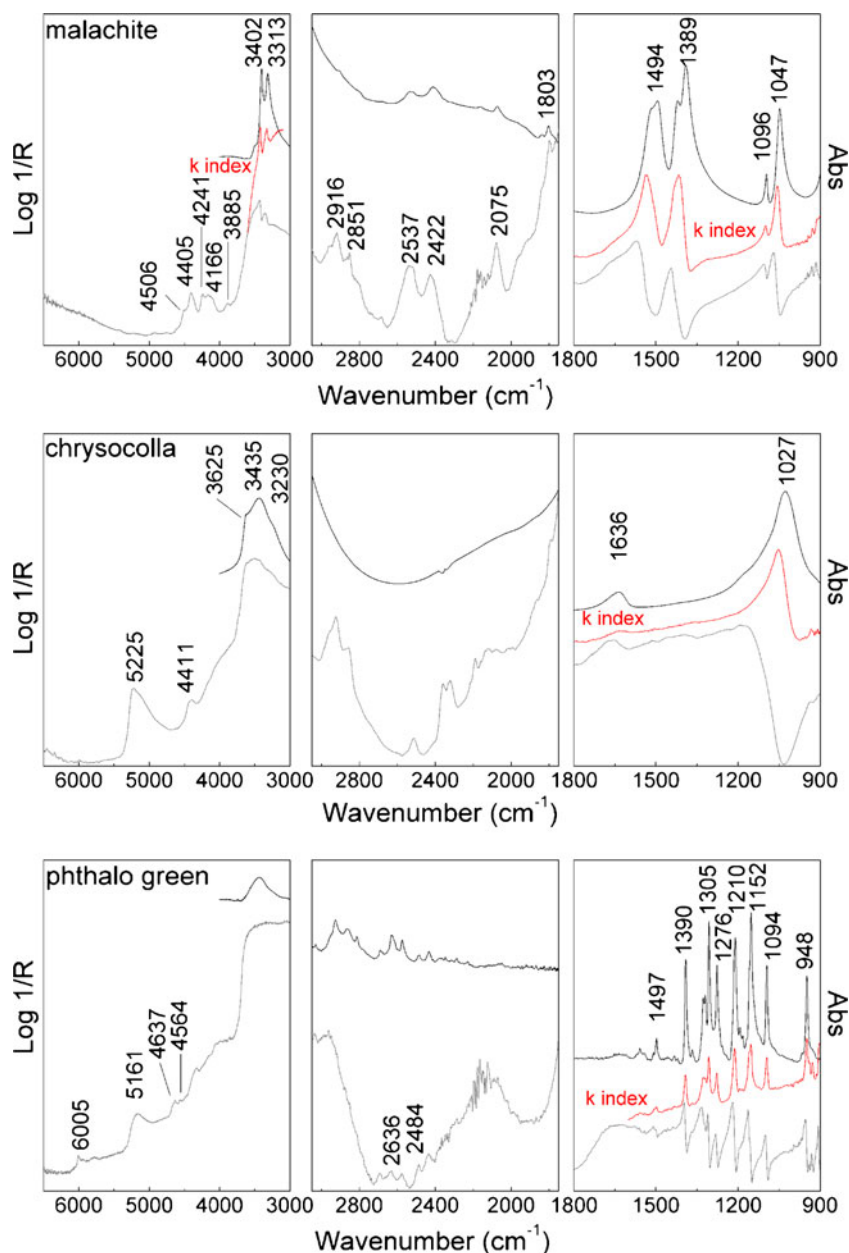
Transmission vs reflection mode spectra of pure green copper-based pigments

To evaluate spectral distortion in reflection mode because of the optical properties of the pigments, conventional transmission spectra were compared with reflection spectra collected from pellets made from pure pigment, for which surface reflection is supposed to be dominant. The total reflection spectra were corrected by KK transformation, by evaluating the effect of this conversion for the main bands and revealing possible discrepancies between the transmission maxima and calculated k index maxima (herein indicated as $\Delta_{\text{KK-}i\nu}$). The spectra are reported in Figs. 1 and 2, and the experimental and calculated values of the maxima are listed in Table 2.

The reflection mode spectrum of malachite shows the fundamental absorption bands of both CO_3^{2-} (Fig. 1) and O–H (Fig. 1) highly distorted. The ν_3 antisymmetric stretching bands of CO_3^{2-} at 1389 and 1494 cm^{-1} are affected by the *reststrahlen* effect and appear as inverted bands (maximum reflection). When the KK correction is applied there is no correspondence among the transmittance maximum frequencies and those occurring in the k index spectrum ($\Delta_{\text{KK-}i\nu} = 30\text{--}40 \text{ cm}^{-1}$). On the other hand, the δ O–H at 1047 cm^{-1} ($\Delta_{\text{KK-}i\nu} = 8 \text{ cm}^{-1}$), the ν_1 of CO_3^{2-} at 1096 cm^{-1} ($\Delta_{\text{KK-}i\nu} = 4 \text{ cm}^{-1}$), and $\nu_3 + \nu_1$ of O–H at 3313 and 3402 cm^{-1} ($\Delta_{\text{KK-}i\nu} = 12\text{--}14 \text{ cm}^{-1}$), appearing as sigmoid bands, are properly corrected.

New characteristic absorptions are visible in the region 1700–2600 cm^{-1} of the reflection mode spectrum (Fig. 1). Considering the molecular structure of malachite, it is reasonable to assign these bands to the following combination and overtone modes typical of carbonate and basic carbonate compounds: 2916 and 2851 cm^{-1} to $2\nu_1$ [20], 2422 and

Fig. 1 Infrared transmission (black line) and reflection (grey line) mode spectra of malachite, chrysocolla, and phthalo green compared with the k index profile obtained from KK correction of the reflection spectra (red line)

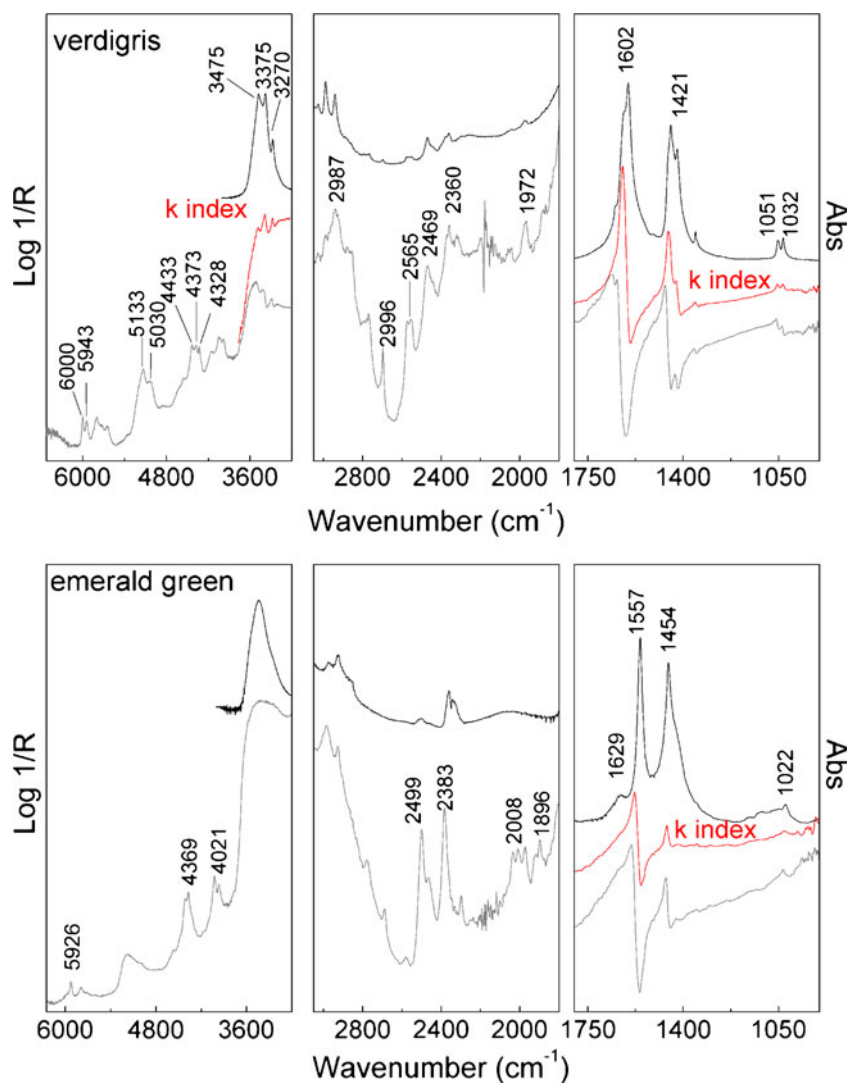


2537 cm^{-1} to $\nu_1 + \nu_3$ [20, 25], 2075 cm^{-1} to 2δ (O–H), and 1803 cm^{-1} (with shoulders at 1768 and 1838 cm^{-1}) to $\nu_1 + \nu_4$. At higher wavenumbers (over 3500 cm^{-1}) further features are visible in the reflection spectrum (Fig. 1). The bands occurring at 4506 and 4405 cm^{-1} can be ascribed to the second-order overtone of $\nu_3 \text{CO}_3^{2-}$, the peaks at approximately 4241 and 4166 cm^{-1} to the combination of O–H bending and stretching, and the band at 3885 cm^{-1} to the combination of the O–H stretching and the Cu–OH deformation modes.

The transmission mode spectrum of chrysocolla, a copper silicate, is shown in Fig. 1. The strongest band at 1027 cm^{-1} is that of Si–O antisymmetric stretching whereas the less intense signal occurring at 1636 cm^{-1} can be ascribed to O–H bending vibration. The O–H stretching region is characterized by a

broad band made of three unresolved components at ca 3230, 3435, and 3625 cm^{-1} . In reflection mode (Fig. 1) the Si–O stretching vibration of this pigment occurs as a strong *reststrahlen* band at 1034 cm^{-1} , the OH bending as a derivative band, and the OH stretching signals as a broad band at 3510 cm^{-1} . The less intense signal at 4411 cm^{-1} can be tentatively assigned to the combination of O–H stretching and Cu–OH deformation and the band at 5226 cm^{-1} to the combination of OH bending and stretching vibrations. As for malachite, the KK correction does not work properly for the strong inverted Si–O mode, giving $\Delta_{\text{KK-}\nu} = 24 \text{ cm}^{-1}$; the correction also affects the shape of the OH stretching which, after the KK correction, appears as a unique broad band centred at 3500 cm^{-1} (Fig. 1).

Fig. 2 Infrared transmission (black line) and reflection (grey line) mode spectra of verdigris and emerald green compared with the k index profile obtained from KK correction of the reflection spectra (red line)



Copper phthalocyanine (Fig. 1) has been already studied and the band assignments in the mid-infrared have been reported elsewhere [26, 27]. In the reflection mode spectrum all the fundamental absorptions of phthalo green between 900 and 1500 cm⁻¹ (Fig. 1) have a derivative shape and are properly corrected by the KK algorithm, as proved by the low $\Delta_{\text{KK-}\nu}$ values reported in Table 2. Also for phthalo green, in the 1700–2600 cm⁻¹ range and over 3500 cm⁻¹, bands attributable to combination and overtone vibrations are visible. The bands between 1700 and 2600 cm⁻¹ are stronger in the transmission spectrum than in the reflection spectrum, probably because the very smooth surface of the phthalo green pellet does not favour the volume reflection.

The reflection spectrum of verdigris (Fig. 2), a neutral copper acetate, is characterized by symmetric and antisymmetric stretching vibrations of the coordinated carboxylate groups at 1421 and 1602 cm⁻¹ respectively [17, 28] appearing as distorted bands. The higher $\Delta_{\text{KK-}\nu}=21$ cm⁻¹ for the first band may suggest a *reststrahlen* character for the stronger antisymmetric stretching whereas the lower $\Delta_{\text{KK-}\nu}=$

9 cm⁻¹ for the symmetric mode indicates a higher contribution of the refraction index in the corresponding reflection spectral profile resembling a derivative band. The O–H stretching vibrations, placed at 3270, 3375, and 3475 cm⁻¹ [28] ($\Delta_{\text{KK-}\nu}=4$ –9 cm⁻¹), have derivative shape. The same distortion ($\Delta_{\text{KK-}\nu}=1$ –9 cm⁻¹) could be seen for the C–H bending modes at 1032, 1051, 1354, and 1444 cm⁻¹. The only non-distorted bands are the less intense bands visible in the 1700–2800 cm⁻¹ range and those appearing over 3500 cm⁻¹. The signals occurring between 3900 and 4200 cm⁻¹ can be assigned to the combination of CH stretching and bending, and the combination of OH stretching and rocking vibrations (at 628 and 690 cm⁻¹ [28], not shown). The three peaks at 4328, 4373, and 4433 cm⁻¹ arise from the combination of CH stretching and bending modes, and the two occurring at 5030 and 5133 cm⁻¹ from the combination of OH stretching and deformation modes. Frost et al. [29], in the spectrum of hoganite, a natural monohydrated copper acetate, assigned bands at 5600 and 5800 cm⁻¹ to the water overtones and those at 5943 and 6000 cm⁻¹ to the first overtone of CH stretching.

Table 2 Experimental maxima and mode assignments of the main absorption bands from the spectra recorded in transmission mode, difference ($\Delta_{\text{KK-t}\nu}$) between the maximum calculated from KK correction of the reflection spectrum and the maximum of the transmission spectrum

Pigment	Frequency (cm^{-1}) (transmission spectrum)	Assignment	Frequency (cm^{-1}) (k index spectrum)	$\Delta_{\text{KK-t}\nu}$ (cm^{-1})	Type of distortion	
Malachite	1047	δ OH	1055	8	Derivative	
	1096	ν_1 CO_3^{2-}	1100	4	Derivative	
	1389	ν_3 CO_3^{2-}	1417	28	Reststrahlen	
	1494	ν_3 CO_3^{2-}	1535	41	Reststrahlen	
	3313	ν OH	3325	12	Derivative	
	3402	ν OH	3416	14	Derivative	
Chrysocolla	1027	ν SiO	1051	24	Reststrahlen	
	1637	δ OH	1638	1	derivative	
Phthalo green	948	δ CH	949	1	Derivative	
	1094	δ CH, η NN	1095	1		
	1152	δ CH	1153	1		
	1159	δ CH	1159	/		
	1183	δ CH, δ NCuN	1183	/		
	1192	δ CH, η NN	1193	1		
	1210	–	1212	2		
	1276	δ CC, δ CH	1277	1		
	1305	η NN, δ CNC, ν CC	1306	1		
	1320	δ CC	1320	/		
	1326	δ CH, ν CC, η NN	1326	/		
	1367	–	1367	/		
	Verdigris	1390	ν CuN, δ CNC	1392	2	
1032		δ CH	1033	1	Derivative	
1051		δ CH	1052	1	Derivative	
1354		δ CH	1356	2	Derivative	
1421		ν_s COO	1425	4	Derivative	
1444		δ CH	1453	9	Derivative	
1601		ν_{as} COO	1621	19	Reststrahlen	
3270		ν OH	3274	4	Derivative	
3375		ν OH	3384	9	Derivative	
3475		ν OH	3482	7	Derivative	
Emerald green		1022	δ CH	1029	7	Derivative
		1454	ν_s COO	1459	5	Derivative
		1556	ν_{as} COO	1577	21	Reststrahlen

The spectrum of emerald green (Fig. 2), a copper acetoarsenite, contains two bands assigned to the carboxylate group at 1454 cm^{-1} (symmetric stretching) and 1557 cm^{-1} (antisymmetric stretching). In this case the KK correction works properly for the weaker symmetric stretching only, with $\Delta_{\text{KK-t}\nu}=5 \text{ cm}^{-1}$; after KK correction the stronger antisymmetric stretching, appearing as a *reststrahlen* band in the reflectance spectrum, is shifted of 21 cm^{-1} relative to the absorption maxima and the resulting spectral shape is quite different from that of a conventional absorption peak.

In conclusion, among the five pigments considered here, only for copper phthalocyanine is the total reflection spectrum properly corrected by use of the KK algorithm. For all the

others there are strong fundamentals bands which appear as *reststrahlen* bands in reflection mode and give large shifts in k index spectra calculated by KK correction. In fact, in correspondence of the *reststrahlen* bands the refractive index may reach values below unity [30], so the condition for the validity of Fresnel's law is lost, and with it the ability of the KK correction to properly correct the distorted spectral profile.

Reflection infrared spectra of green copper-based pigments on model paintings

In general, the presence of both proteinaceous and lipid binders substantially affects the infrared fingerprint regions

showing, in this range, characteristic signals. Specifically, the three strong signals assigned to amide I at 1657 cm^{-1} , amide II at 1549 cm^{-1} , and amide III at 1446 cm^{-1} from the protein, and C–O stretching vibrations at 1099 , 1170 , and 1242 cm^{-1} , C–H bending vibrations at 1376 and 1460 cm^{-1} , and C=O stretching vibration at ca 1740 cm^{-1} from the lipid may overlay the diagnostic bands of Cu-based pigments.

The spectra of malachite mixed with different concentrations of the two binders are reported in Fig. 3 to illustrate further considerations regarding the spectral modifications arising in reflection mode and the possibility of applying the KK correction.

In more detail, the position of the minima of the fundamental bands, for example $\delta\text{ OH}$ at 1047 cm^{-1} and $\nu_3\text{ CO}_3^{2-}$

at 1389 and 1494 cm^{-1} (indicated by the dotted line in Fig. 3) depend on the pigment-to-binder ratio. Considering the minimum of the inverted band in the pure powder spectrum compared with the painting model spectra, the hydroxyl bending is shifted by $1\text{--}4\text{ cm}^{-1}$ in tempera mock-ups and by $16\text{--}19\text{ cm}^{-1}$ in oil mock-ups whereas the anti-symmetric stretching signals of the carbonate is shifted by $2\text{--}7\text{ cm}^{-1}$ in tempera mock-ups and by $18\text{--}34\text{ cm}^{-1}$ in oil mock-ups. Applying the KK correction to the spectra obtained from models with higher concentrations of malachite (pigment-to-binder 3:1), the $\Delta_{\text{KK-t}\nu}$ of the mock-ups is always higher than that observed for the pure pigment (22 cm^{-1} for hydroxyl bending and 48 and 58 cm^{-1} for the two carbonate stretching peaks for the tempera model; 42 and 44 and 71 cm^{-1} for the oil model). Furthermore, for both the binders $\Delta_{\text{KK-t}\nu}$ increases as the concentration of the pigment decreases.

The KK correction does not work properly for complex systems, for example the model paintings, for which the surface reflection is not the only contribution to the total reflection. In the painting models, in fact, the pigment particles are diluted in the binder, favouring penetration of the radiation and thus generating a volume reflection also.

The fact that the $\Delta_{\text{KK-t}\nu}$ is higher for the oil mock-ups than for the tempera mock-ups may have different explanations, both related to the different optical properties of the surfaces in terms of refraction index, surface morphology, and a different pigment–binder mixture that can be more or less homogeneous.

Having very low k indexes, the combination and overtone bands are barely affected by the total reflection, being only enhanced and not shifted or distorted. The $2\delta(\text{OH})$, the $\nu_1+\nu_3\text{ CO}_3^{2-}$ and the $\nu_1+\nu_4\text{ CO}_3^{2-}$ (Fig. 3, indicated by hash marks) already appear in 1:1 ratio with casein whereas in the oil mock-ups the first two arise in 2:1 ratio and the latter is never visible, probably because of the strong effect of the $\nu\text{ C=O}$ of the lipid binder. With the highest amount of binder (pigment-to-binder 1:2, either protein and lipid) only the high-wavenumber combination and overtone modes of malachite can be used for diagnostic purposes. In more detail, the $2\delta(\text{OH})$ and the signals over 3700 cm^{-1} (at 4241 , 4405 , and 4506 cm^{-1}) are visible in both spectra (Fig. 3, indicated by asterisks), the last ones partially overlapped with the CH combination band of oil, however.

For the other tempera and oil model paintings (Figs. 4 and 5), the following observations were made.

- Chrysocolla, whose infrared spectrum is characterized by few signals, was undetectable when mixed with both binders;
- In the verdigris tempera model, only the carboxylate antisymmetric stretching COO^- is clearly visible, but shifted approximately 7 cm^{-1} relative to the pure

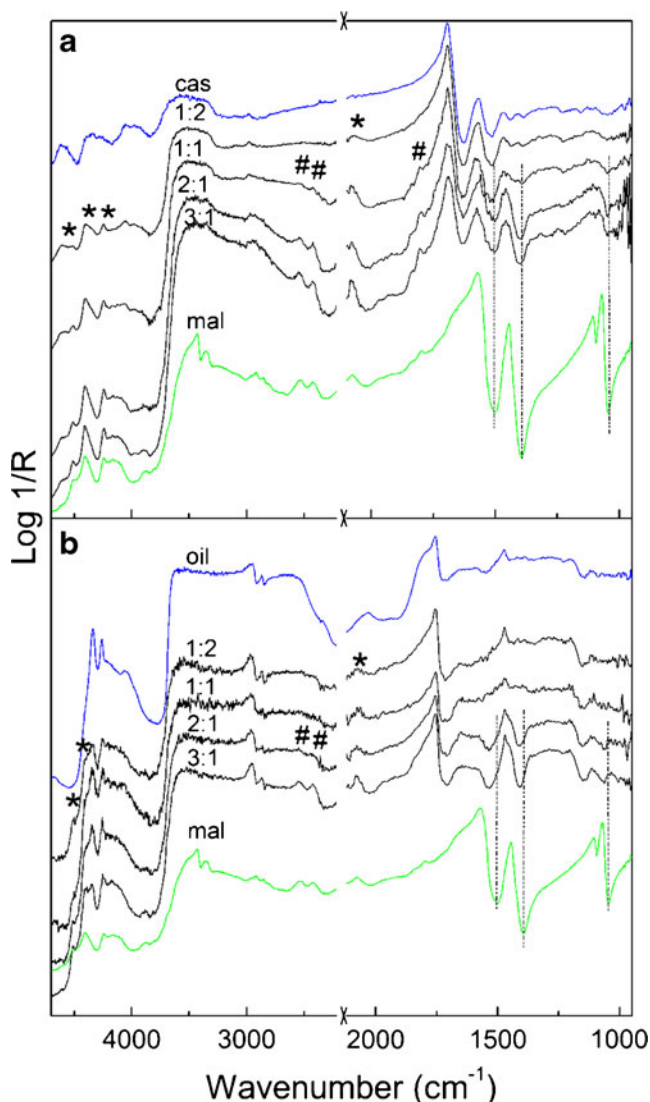
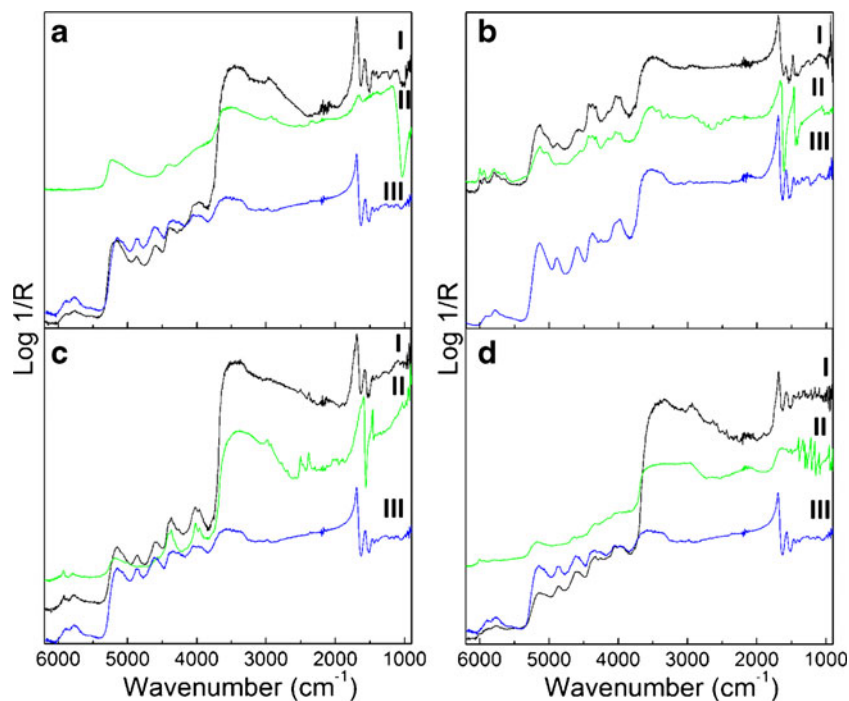


Fig. 3 Infrared reflection spectra of malachite models with different pigment-to-binder ratios for casein (a) and oil (b). Pure binder (blue line), pigment + binder (black line), and pure pigment (green line). Combination and overtone bands are highlighted by asterisks and hash marks, respectively

Fig. 4 FTIR reflection spectra of the tempera models: (a) chrysocolla, (b) verdigris, (c) emerald green, (d) phthalo green. Pigment + binder (I, black line), pure pigment (II, green line), and binder (III, blue line)



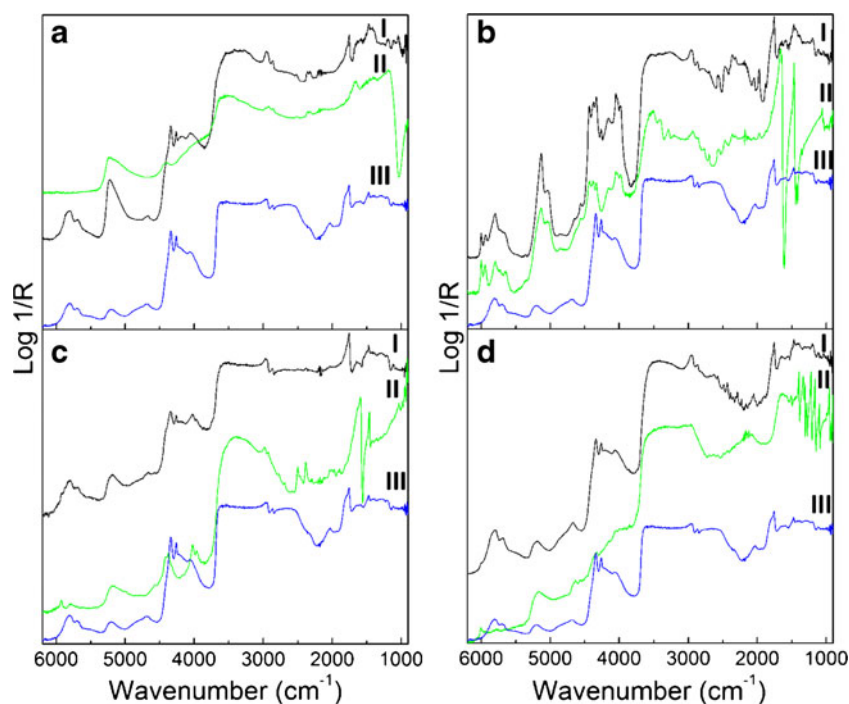
pigment; on applying the KK correction $\Delta_{\text{KK-t}\nu}$ is 38 cm^{-1} . The combination and overtone bands between 1700 and 2800 cm^{-1} are not visible, whereas those occurring in the near infrared above 3500 cm^{-1} are still observable. In the oil mock-up, no fundamental bands appear in the spectrum, but all the less intense combination and overtone signals are well defined.

- In the emerald green tempera mock-up, only the combination and overtone bands are visible. In the oil mock-

up, in addition to these, the inverted antisymmetric stretching COO^- is also detectable and it shifts from 1558 to 1570 cm^{-1} with relative to the pure pigment (considering the minimum of the inverted bands).

- In the phthalo green mock-ups, the fundamental features of the green pigment fall in a spectral range where there is no overlapping with the proteinaceous binder, resulting in the visualization of derivative-like bands. In the oil model, the fundamental bands of the green pigment

Fig. 5 Infrared reflection spectra of the oil model samples: (a) chrysocolla, (b) verdigris, (c) emerald green, (d) phthalo green. Pigment + binder (I, black line), pure pigment (II, green line), and binder (III, blue line)



are mainly masked by strong lipid signals. Despite this, the infrared range of the combination bands and overtone bands ($2000\text{--}3000\text{ cm}^{-1}$) being free from the binder signals can be used to identify phthalo green in the presence of the oil. It is interesting to note for the tempera mock-up that after use of the KK algorithm $\Delta_{\text{KK-}i\nu}$ is approximately $1\text{--}2\text{ cm}^{-1}$, in agreement with the results obtained by applying the KK correction to the pellet spectrum.

In conclusion, study of the model samples demonstrated that all the copper-based pigments but chrysocolla can be non-invasively identified by reflection FTIR when considering as diagnostic features the combination and overtone bands that differ from the fundamental band being not distorted by matrix effects.

Analysis of original paintings and manuscripts

In general, the identification of malachite on different types of artworks (manuscripts, murals, easel paintings) was found to be quite straightforward using the mid infrared carbonate combination and hydroxyl overtone bands which are enhanced by diffuse reflection and are not masked by signals of the paint matrix.

To give an example, infrared spectra of green areas obtained from miniatures (Fig. 6a, b) of the three illuminated manuscripts are shown in Fig. 6c, in which the peculiar shape of the $\nu_1 + \nu_3$ combination bands of CO_3^{2-} at 2525 and 2425 and the $2\delta(\text{OH})$ at 2075 cm^{-1} of malachite are visible. The near IR combination bands at 4400 and 4245 cm^{-1} (Fig. 6c) are also observable in the two spectra, although partially overlapping with the binder and support infrared signals. Furthermore, in this particular case study some of the fundamental bands are also detectable— CO_3^{2-} asymmetric stretching at 1385–1490 cm^{-1} and OH bending at 1043 cm^{-1} .

In Perugino's mural painting, a mixture of green and blue copper carbonate pigments (Fig. 7) was detected by non-invasive FTIR analysis [31]. In fact, azurite has been identified in the shadows of the darker areas of the green mantle ($\nu_1 + \nu_3$ of CO_3^{2-} at 2550 and 2501 cm^{-1}) which were made with malachite ($\nu_1 + \nu_3$ of CO_3^{2-} at 2423 cm^{-1} and $2\delta(\text{OH})$ at 2078 cm^{-1}). In Fig. 7b, in which the spectral range of interest for the combination bands is enlarged, it can be noted that the features of both copper carbonates can be differentiated from those of the calcium carbonate matrix lying in the same spectral region.

Notably, the combination and overtone bands used as markers for identification of malachite are clearly seen in the spectrum recorded on a varnished area of a panel painting by Niccolò di Liberatore (Fig. 8, III), albeit with a more noisy profile than the spectrum recorded on the same green

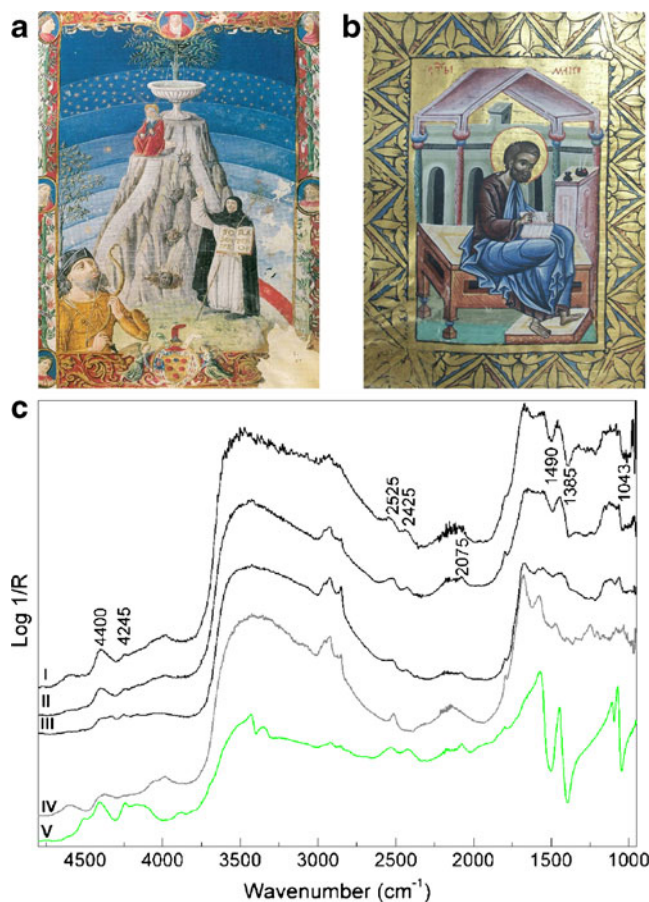


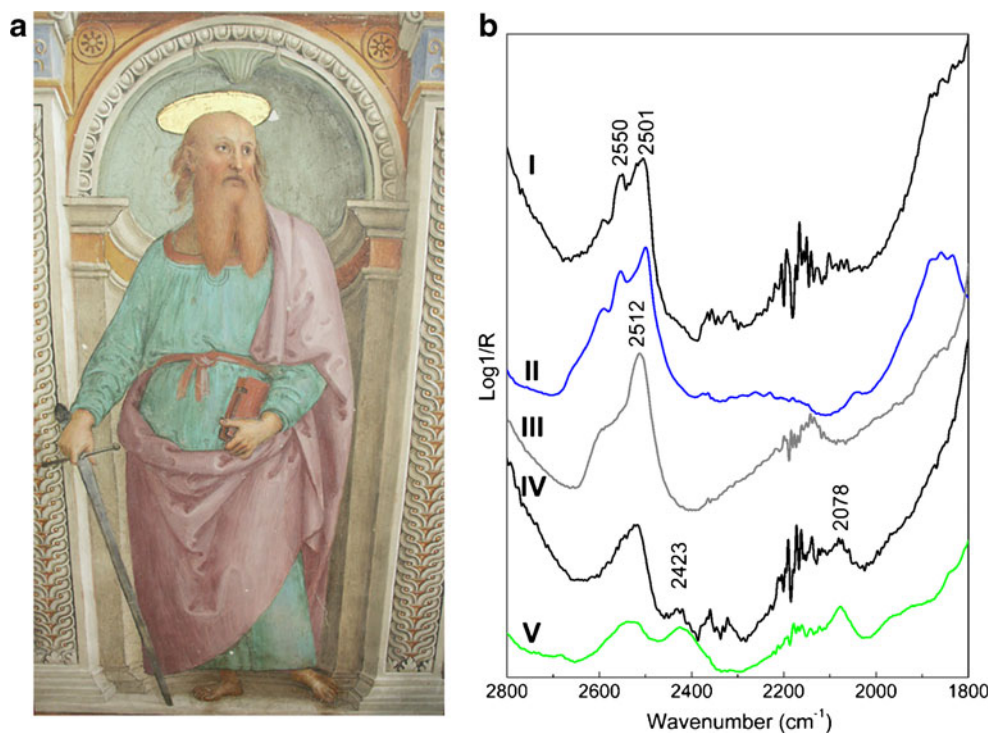
Fig. 6 (a) *Anima Pellegrina* by Tommaso Sardi, miniature of the Palazzo Corsini manuscripts. (b) Miniature of one of the Putna monastery gospels. (c) FTIR reflection spectra recorded on green areas of the illuminated manuscripts: I, *Anima Pellegrina*; II, p. 121 St Mark's Gospel; III, p. 185 St Luke's Gospel; IV, parchment; V, malachite standard

area but unvarnished because under the picture frame (Fig. 8, II).

Use of emerald green in the Munch and Boccioni paintings (Fig 9a,b) was first suggested by detection of As and Cu in the XRF measurements; it was then confirmed on the basis of the combination and overtone bands occurring at 3960, 4015, and 4411 cm^{-1} and the carboxylate antisymmetric stretching at 1570 cm^{-1} (minimum of inverted band, as discussed for models) (Fig. 9c).

Identification of verdigris was much more challenging; as a matter of fact, it has never been detected for certain by use of infrared reflection mode either on paintings [3] or on illuminated manuscripts, for which, in particular, according to ancient writings, it was widely used. Considering that such difficulties have not emerged in this work in the study of unaged model paints, explanation must be found in the low stability of copper acetates which have been proved to undergo carboxylate–acetate ligand exchange when mixed with lipid binding medium [32]. The copper-based green on

Fig. 7 (a) Detail of Perugino's fresco *Adorazione dei Pastori*. (b) FTIR reflection spectra recorded from the green robe of Saint Paul: *I*, blue shadow; *II*, azurite standard; *III*, mortar; *IV*, green shadow; *V*, malachite standard

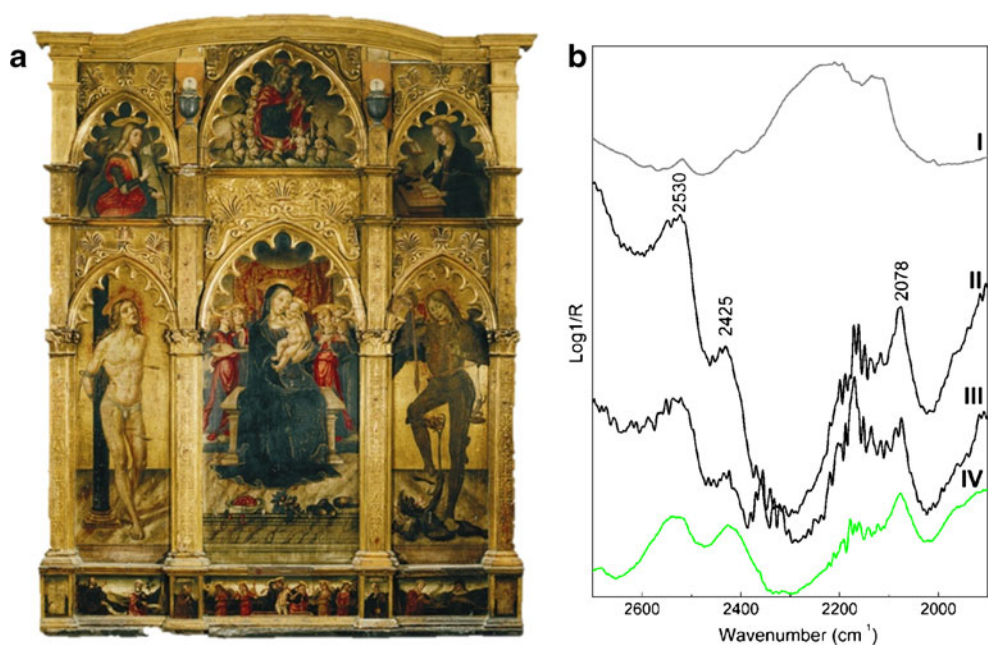


The Crucifixion of Christ (Fig. 10a), which has degraded to a brownish colour over much of the painting, was suggested to be verdigris-type by FTIR microscopy of micro-samples [33]. Non-invasive reflection spectra recorded on areas in which the green colour has been preserved (Fig. 10b) show, besides bands related to the canvas, a sharp and inverted band at 1586 cm^{-1} that could be assigned to copper fatty-acid soaps [34] also detected on related micro-samples [33]. It is worth mentioning that XRF measurements, performed on different green areas of the same painting, have revealed

the presence of chlorine associated and linearly correlated with copper (Fig. 10c), indicative of the presence of verdigris, because some recipes for verdigris recommended use of chlorides [35].

Alteration of verdigris, ground in a oil medium, with formation of amorphous copper fatty acid soaps, has been proved for ancient easel paintings by micro-FTIR analysis on micro samples, by identification of COO^- antisymmetric and symmetric stretching at approximately 1585 and 1411 cm^{-1} , respectively [36–38]. Copper oxalate, also, has

Fig. 8 (a) Niccolo Liberatore's panel painting *Polittico di Sant' Angelo*. (b) FTIR reflection spectra recorded from: *I*, ground layer; *II*, unvarnished green area under the picture frame; *III*, varnished green area; *IV*, malachite standard



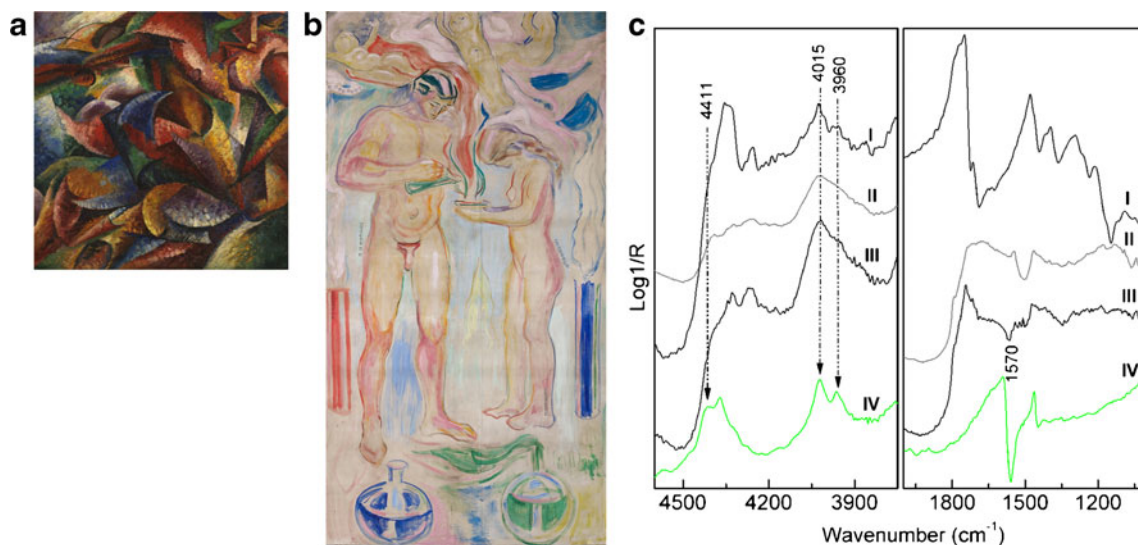


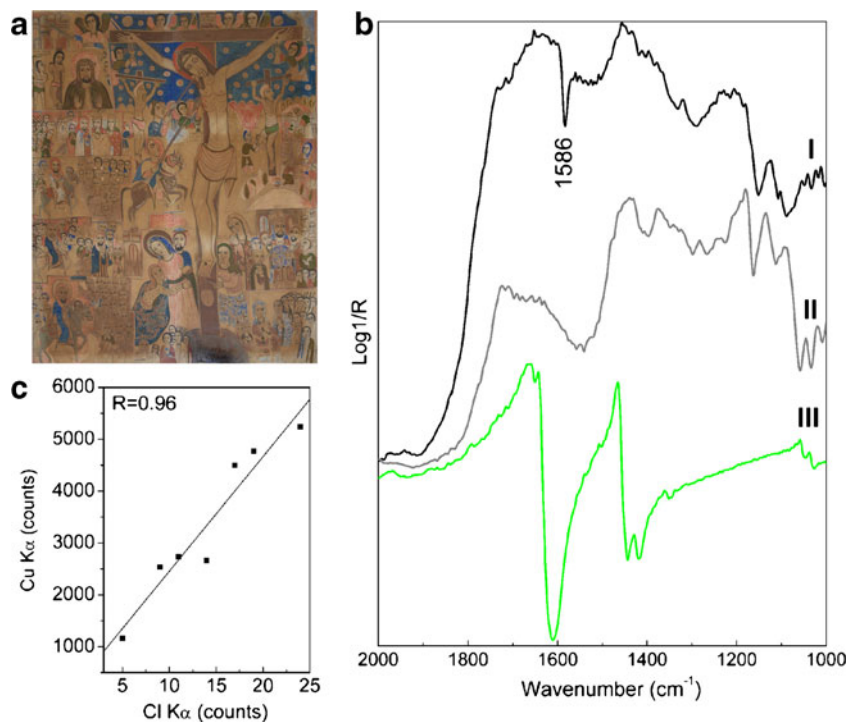
Fig. 9 (a) *Dinamismo di un corpo umano*, Umberto Boccioni's painting on canvas. (b) *Chemistry* Edvard Munch's painting on canvas. (c) FTIR reflection spectra recorded from green areas: *I*, green area from

the Boccioni painting; *II*, canvas; *III*, green area from the Munch painting; *IV*, emerald green standard

been identified on copper-based green areas of easel paintings, mural paintings, ceramics, and maps by use of micro-X-ray diffraction [37], micro-Raman [39, 40] or micro-FTIR in laboratories [39] and by portable FTIR in-situ [12].

A systematic study of the effect of thermal and photochemical aging on the infrared spectral behaviour of different Cu-based pigments mixed with oil and proteins is in progress, with the purpose of evaluating which spectral modifications can be encountered for each of these on original objects.

Fig. 10 (a) Ethiopian painting on canvas *The Crucifixion of Christ* (1855–1893). (b) FTIR reflection spectra recorded from green areas: *I*, green area; *II*, canvas; *III*, verdigris standard. (c) XRF counts measured for chlorine (K_{α}) and copper (K_{α}) on green areas showing the correlation between the two



Conclusions

This paper illustrates the potential of FTIR reflection spectroscopy for in-situ molecular identification of copper-based green pigments. Analysis conducted on pellet samples revealed spectral distortions and modifications observed when working in reflection mode compared with conventional infrared transmission, and revealed useful diagnostic bands for identification purposes. Application of the Kramers–Kronig correction to spectra acquired from the

pure pigments, as pellets, to correct for the distortion arising from the surface reflection, gave reliable spectral features for the derivative-like profiles, whereas for *reststrahlen* bands originating from the antisymmetric band of the different copper ligands (carbonate, acetate, and silicate) it gave k index maxima shifted by approximately 20–40 cm^{-1} relative to those obtained in transmission mode. These findings stress the need to carefully manage the KK correction for reflection spectra, to avoid misleading interpretation and erroneous assignment.

The results obtained for mock up painting samples showed that different binders do not prevent the visualization of pigment diagnostic bands even when working in reflection mode, the only exception being chrysocola, the copper silicate, whose reflection spectrum is characterized solely by a *reststrahlen* band at approximately 1027 cm^{-1} and a few small and unspecific combination bands all overlaid by the signals from the organic binding media.

The knowledge gained by studying the pure pigments and the paint models in reflection mode was used for assignment of infrared spectra collected in-situ for paintings and manuscripts painted with malachite, emerald green, and verdigris. As was already apparent from the study of models, the use of combination and overtone bands related to the fundamental stretching and/or bending of copper ligands enabled certain identification of both malachite and emerald green in different types of paintings, even in the presence of varnish. In contrast, the identification of verdigris was far from easy, most likely not because of overlapping of matrix signals or spectral distortions but because of dissolution, over time, of neutral and/or basic copper acetates in the binder, which resulted in the observation of a new band assigned to antisymmetric stretching of copper fatty acid soaps.

Acknowledgments The EU programmes Eu-ARTECH (FP6, <http://www.eu-arteche.org>) and CHARISMA (FP7, <http://www.charismaproject.eu>) and the Italian MIUR (PRIN08, *Materiali e sistemi innovativi per la conservazione dell'arte contemporanea* 2008 FFXXN9) are acknowledged for financial support. Thanks are expressed to the staff of the British Museum, Palazzo Corsini, Putna Monastery, Museo del Novecento, Conservation Studies, Department of Archaeology, Conservation and History (University of Oslo), and Sovrintendenza per i Beni Artistici Storici ed Etnoantropologici dell'Umbria for agreeable cooperation.

References

- Miliani C, Rosi F, Brunetti BG, Sgamellotti A (2010) *Acc Chem Res* 43:728–738
- Clementi C, Ciocan V, Vagnini M, Doherty B, Laurenzi Tabasso M, Conti C, Brunetti BG, Miliani C (2011) *Anal Bioanal Chem* 401:1815–1826
- Van der Snickt G, Miliani C, Janssens K, Brunetti BG, Romani A, Rosi F, Walter P, Castaing J, De Nolf W, Klaassen L, Labarque I, Wittermann R (2011) *J Anal At Spectrom* 26:2216–2229
- Aceto M, Agostino A, Fenoglio G, Gulmini M, Bianco V, Pellizzi E (2012) *Spectrochim Acta A* 91:352–359
- Colomban P, Tournié A, Caggiani MC, Paris C (2012) *J Raman Spectrosc*. doi:10.1002/jrs.4101
- Delaney JK, Zeibel JG, Thoury M, Littleton R, Palmer M, Morales KM, de la Rie ER, Hoenigswald A (2010) *Appl Spectrosc* 64:584–594
- Rosi F, Miliani C, Clementi C, Kahrim K, Presciutti F, Vagnini M, Manuali V, Daveri A, Cartechini L, Brunetti BG, Sgamellotti A (2010) *Appl Phys A* 100:613–624
- Bacci M, Casini A, Cucci C, Piccolo M, Radicati B, Vervat M (2003) *J Cult Herit* 4:329–336
- Rosi F, Manuali V, Grygar T, Bezdzicka P, Brunetti BG, Sgamellotti A, Burgio L, Seccaroni C, Miliani C (2011) *J Raman Spectrosc* 42:407–414
- Schmidt CM, Trentelman KA (2009) *PS* 6:10–21
- Deneckere A, Leeflang M, Bloem M, Chavannes Mazel CA, Vekemans B, Vincze L, Vandenabeele P, Moens L (2011) *Spectrochim Acta A* 83:194–199
- Miliani C, Doherty B, Daveri A, Loesch A, Ulbricht H, Brunetti BG, Sgamellotti A (2009) *Spectrochim Acta A* 73:587–592
- Duran A, Perez-Rodriguez JL, Espejo T, Franquelo ML, Castaing J, Walter P (2009) *Anal Bioanal Chem* 395:1997–2004
- Irazola M, Olivares M, Castro K, Maguregui M, Martínez-Arkarazo I, Madariaga JM (2012) *J Raman Spectrosc*. doi:10.1002/jrs.4036
- Vandenabeele P, Lambert K, Matthys S, Schudel W, Bergmans A, Moens L (2005) *Anal Bioanal Chem* 383:707–712
- Gettens RJ (1993) In: West Fitzhugh E, Roy A (eds) *Artists' Pigment—A handbook of their history and characteristics vol. 2*. National Gallery of Art of Washington in association with Oxford University Press, New York, London, pp 183–202
- Kunn H (1993) In: Roy A (ed) *Artists' Pigment—A handbook of their history and characteristics vol. 2*. National Gallery of Art of Washington in association with Oxford University Press, New York, London, pp 131–158
- Eastaugh N, Walsh V, Chaplin T, Siddall R (2004) *Pigment compendium—A dictionary and optical microscopy of historical pigments*. Elsevier, Elsevier Butterworth-Heinemann, Oxford
- Fiedler I, Bayard M (1997) In: West Fitzhugh E (ed) *Artists' Pigment—A handbook of their history and characteristics vol. 3*. National Gallery of Art of Washington in association with Oxford University Press, New York, Oxford, pp 219–293
- Miliani C, Rosi F, Daveri A, Brunetti BG (2012) *Appl Phys A* 106:295–307
- Griffiths P, De Haseth JA (2007) *Fourier transform infrared spectrometry*, 2nd edn. Wiley, New York
- Rosi F, Daveri A, Doherty B, Nazzareni S, Brunetti BG, Sgamellotti A, Miliani C (2010) *Appl Spectrosc* 64:956–963
- Vetter W, Schreiner M (2011) *PS* 8:10–22
- Poli T, Chiantore O, Nervo M, Piccirillo A (2011) *Anal Bioanal Chem* 400:1161–1171
- Ricci C, Miliani C, Brunetti BG, Sgamellotti A (2006) *Talanta* 6:1221–1226
- Li D, Peng Z, Deng L, Shen Y, Zhou Y (2005) *Vib Spectrosc* 39:191–199
- Barszcz B, Bogucki A, Biadasz A, Bursa B, Wrobel D, Graja A (2011) *J Photochem Photobiol A* 218:48–57
- Cartechini L, Miliani C, Brunetti BG, Sgamellotti A, Altavilla C, Ciliberto E, D'Acapito F (2008) *Appl Phys A* 92:243–250
- Musumeci A, Frost RL (2007) *Spectrochim Acta A* 67:48–57
- Korte EH, Röseler A (2005) *Anal Bioanal Chem* 382:1987–1992
- Miliani C, Rosi F, Borgia I, Brunetti BG, Sgamellotti A (2007) *Appl Spectrosc* 61:293–299
- Gunn M, Chottard G, Riviere E, Girerd J, Chottard J (2002) *Stud Conserv* 47:12–23
- Cutts H, Harrison L, Higgitt C, Cruickshank P (2010) *Brit Mus Tech Res Bull* 4:1–17

34. Robinet L, Corbeil MC (2003) *Stud Conserv* 48:23–40
35. Favaro M, Vigato PA, Andreotti A, Colombini MP (2005) *J Cult Herit* 6:295–305
36. Salvado N, Buti S, Tobin MJ, Pantos E, Prag AJNW, Pradell T (2005) *Anal Chem* 77:3444–3451
37. Salvado N, Buti S, Nicholson J, Emerich H, Labrador A, Pradelle T (2009) *Talanta* 79:419–428
38. Spring M, Higgitt C (2006) In: Nadolny J (ed) *Medieval painting in Northern Europe: Techniques, analysis, art history*. Archetypes Publication, London, pp 223–229
39. Nevin A, Loring Meli J, Osticioli I, Gautier G, Colombini MP (2008) *J Cult Herit* 9:154–161
40. Mendes N, Lofrumento C, Migliori A, Castellucci EM (2008) *J Raman Spectrosc* 39:289–294